

Characterization of Process Induced Surface Profiles and Lattice Strains using Optical Surface Profilometry and Multi-wavelength Raman Spectroscopy

Woo Sik Yoo*, Takeshi Ueda, Junya Kajiwara, Toshikazu Ishigaki and Kitaek Kang

WaferMasters, Inc.
246 East Gish Road, San Jose, CA 95112 U.S.A.

In-line process monitoring plays a vital role in quickly identifying and resolving yield problems in semiconductor manufacturing environments. It is also a very important and powerful methodology in the understanding of material properties during process development and accelerating yield ramps in smaller scale devices. We have developed non-destructive, in-line process and/or material property monitoring methods which use reflection, diffraction and scattering of laser beams. Process induced changes of surface profiles and lattice strains are characterized using newly developed optical surface profilometry (OSP) and multi-wavelength Raman spectroscopy (MRS) systems. Optical surface profiles and Raman characterization were performed on Ni films on 300mm p⁻-Si wafers with or without TiN capping layers, before and after annealing in addition to the conventional sheet resistance measurement using a four point probe. Significant changes in wafer surface profiles and strains near the Ni/Si interface were observed near phase transition (Ni/Si→Ni₂Si→NiSi→NiSi₂) temperatures as determined by the temperature sensitivity curve of sheet resistance.

Introduction

A wafer goes through global and local surface profile and strain (or stress) changes during various process steps due to chemical reactions and physical changes under a specific (uniform or non-uniform) process environment. In general, global flatness is strongly desired for preventing pattern overlay problems in photolithography steps [1]. In some cases, such as SiGe/Si, intentional local strain generation is desired for enhancing device performance [2]. Process induced local strain and/or deformation of surface flatness can cause focusing problems in photolithography steps and results in pattern overlay problems and critical dimension errors in nanometer scale devices [1]. Just like process results, characterizing, understanding and managing process induced surface profiles and lattice strains are becoming extremely important for nanometer scale device manufacturing.

For more than a decade, in-line process monitoring technology has been introduced in device manufacturing environments and plays a vital role in quickly identifying and resolving yield problems. Many different types of in-line process

* Contact Author: e-mail: woosik.yoo@wafermasters.com, phone: +1-408-451-0856

monitoring methods and tools for measurement of film thickness, sheet resistance, and particles on blanket wafers have been implemented. The non-destructive nature of the in-line process monitoring technology makes it attractive. However, the development of non-destructive and non-contact optical characterization tools for patterned production wafers can be quite difficult due to the interference between the light source and small geometry patterns with dimensions close to that of the light source wavelength.

In this paper, process induced surface profiles and lattice strains, along with process results on 300mm blanket and device wafers are characterized before and after thermal processing.

Experiment

TiN (~10nm thick) capped, nickel (Ni) films (~30nm thick) on (100) oriented p-type 300mm blanket and patterned silicon (Si) wafers were prepared. Si wafers with Ni film were annealed in the temperature range of 200~425°C using a hotplate-based, low temperature annealing system (WaferMasters Stacked Anneling Oven (SAO-300LP)). All wafers were annealed in N₂ at 1 atmosphere for 10min. in the following manner. The wafer is placed on three small standoffs between heated aluminum hotplates without touching the hot plates (Fig. 1). The distance between the wafer and (top and bottom) hotplates is kept at 10mm during annealing. Since conduction and convection are the dominant heat transfer mechanisms in this temperature range (200°C~425°C), compared to radiation, wafers are annealed gently, as the wafer approaches a saturation temperature provided by the top and bottom hotplates. A detailed configuration of the annealing system and its thermal characteristics is published elsewhere [3 - 5].

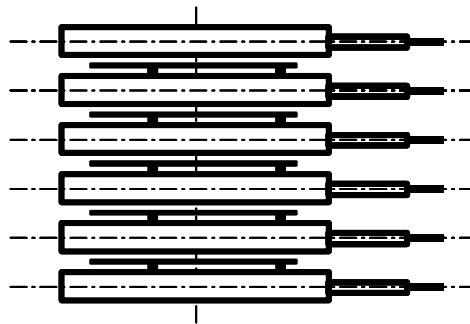


Figure 1. Schematic illustration of wafers between stacked hotplates.

To understand the potential impact of macroscopic and microscopic temperature non-uniformity and non-repeatability, electrical and optical properties of TiN/Ni films on blanket and patterned wafers were measured as a function of annealing temperature. Any process induced surface profiles and lattice strains of wafers, before and after thermal

processing are non-destructively characterized using WaferMasters OSP-300 (Optical Surface Profilometry) and MRS-300 (Multi-wavelength Raman Spectroscopy) systems.

Results and Discussions

Electrical Characterization by Four Point Probe

Changes in sheet resistance after annealing of TiN (~10nm thick) capped ~30nm thick Ni films sputtered on p-type Si wafers were measured using a four point probe and plotted as a function of annealing temperature. Sheet resistance measurements were done at 225 points per wafer excluding 3mm from the wafer edge. Figure 2 shows the sensitivity of sheet resistance to annealing temperature for TiN capped Ni films undergoing 300s annealing.

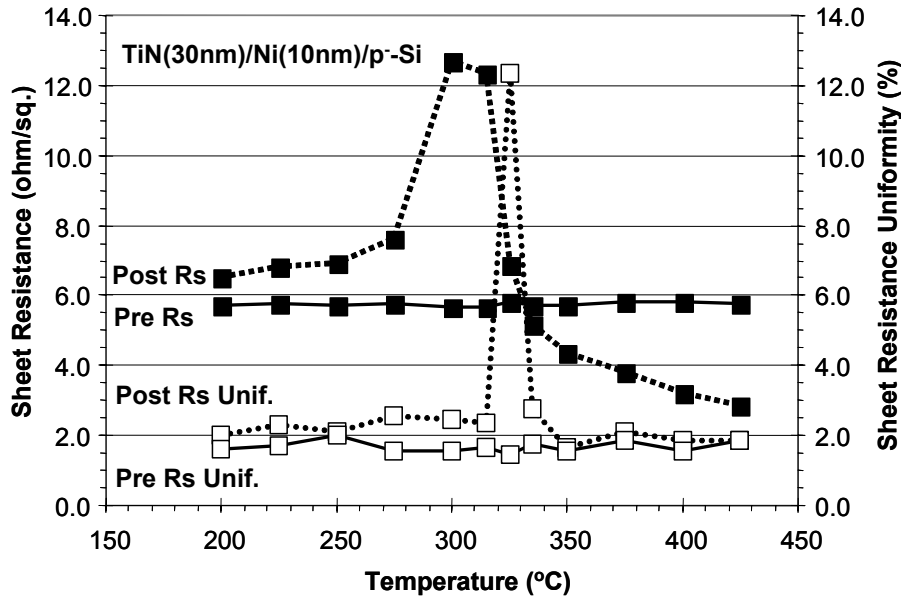


Figure 2. Sheet resistance and sheet resistance uniformity of TiN/Ni films on p-type Si before and after annealing at different temperatures.

Sheet resistance and uniformity, as deposited, under sputtering condition A are ~5.7ohm/sq. and ~2.0% in 1σ before annealing. At 200°C, the sheet resistance increased from ~ 5.7ohm/sq. (as-deposited TiN capped nickel film on Si) to ~ 6.5ohm/sq. by slightly forming the high resistivity, Ni-rich silicide phase (Ni_2Si). Between 275°C and 300°C, the sheet resistance sharply increased to ~12.7ohm/sq. as the phase transition from low resistivity metallic Ni phase to the high resistivity Ni-rich Ni_2Si phase was completed. As annealing temperature continues to increase, the sheet resistance sharply decreases from >12ohm/sq. reaching ~2.8ohm/sq. at 425°C as the phase transition from

the high resistivity Ni-rich Ni_2Si phase to a lower resistivity, stoichiometric NiSi phase takes place. Sheet resistance uniformity remained constant at $\sim 2.0\%$ except for the phase transition temperature of $\sim 325^\circ\text{C}$.

Process Induced Surface Profile Change Characterized by OSP-300

The Optical surface profilometry (OSP-300) system irradiates a wafer with a laser beam at a fixed incident angle and captures reflected, diffracted and scattered images from the wafer to characterize the wafer surface profile and pattern distortions. The system generates wafer maps of vector plots, intensity, height contours, and distortion. It also generates the height profile and estimated curvature along the major crystal orientations as well as a histogram of wafer surface misorientation from the wafer stage. By comparing wafer surface profiles before and after a certain process step or a series of process steps, for both blanket and patterned production wafers, process induced surface profiles can be estimated and the accumulated impact of these process steps on the wafer's surface profile can be generated as wafer maps.

Figure 3 shows vector plot, height map, variation and curvature along major crystal orientations obtained by the OSP-300 system and sheet resistance maps from TiN capped Ni films on Si wafers after annealing at 300, 315, 325 and 335°C for 300s in an SAO-300LP system. As seen in Figs. 2 and 3, sheet resistance sharply dropped from 12.68ohm/sq. to 5.15ohm/sq. in the annealing temperature range of 300°C and 335°C due to the phase transition from the high resistivity Ni-rich Ni_2Si phase to a lower resistivity, stoichiometric NiSi phase. The sheet resistance map from the wafer annealed at 325°C showed large sheet resistance variations (high Rs uniformity of 12.36%) due to an incomplete $\text{Ni}_2\text{Si} \rightarrow \text{NiSi}$ phase transition. Wafer surface profiles measured using the OSP-300 system also indicate that the wafer surface profile is heavily distorted by the incomplete $\text{Ni}_2\text{Si} \rightarrow \text{NiSi}$ phase transition. The curvature along two ($[010]$ and $[-100]$) out of four major crystal orientations became concave from convex. Once the $\text{Ni}_2\text{Si} \rightarrow \text{NiSi}$ transition is nearly completed, at 335°C , sheet resistance uniformity improved and the wafer surface profile became flatter. The curvature along all major crystal orientations again became convex.

Optical surface profile measurement allows one to directly visualize the impact of a process on global and local wafer distortion along with wafer profile and estimated wafer curvature along major crystal orientations. The symmetry of reaction and preferred orientation for a certain reaction can be determined from the optical surface profile data. A nickel silicidation process modulates stress at the Ni/Si interface on the front side of a wafer and affects the wafer surface topology by distributing that local stress over the wafer.

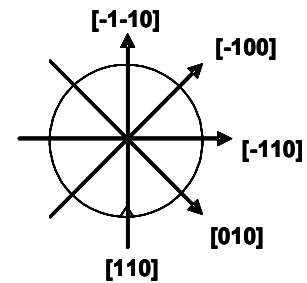
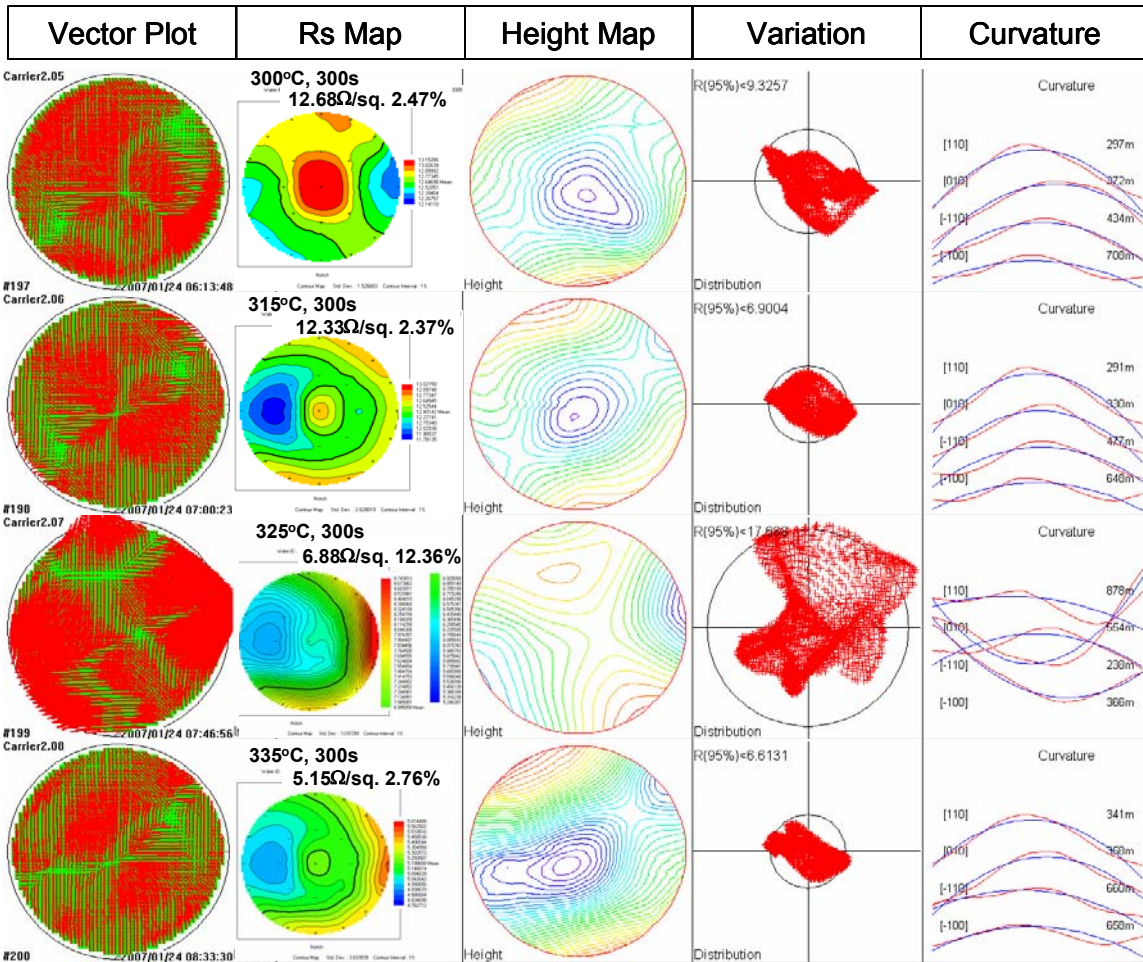


Figure 3. Wafer surface profile and sheet resistance (Rs) maps of TiN/Ni deposited 300mm diameter Si wafers after annealing at various temperatures in N₂.

Optical properties of patterned wafers are much different from those of blanket wafers. Patterned wafers are generally very reflective and diffract light. Figure 4 shows a typical diffraction pattern from a device wafer under laser beam irradiation perpendicular to the wafer surface. The diffraction pattern under laser illumination is a signature of the wafer device patterns. The behaviors of patterned wafers are quite similar to diffraction gratings used in monochromators. The diffraction gratings have a large number of

parallel grooves in one direction. The groove density varies from hundreds to thousands lines/mm depending on the wavelength of interest. The distance between grooves is in the range of a few μm to a few hundred nm. Patterned product wafers have features of various shapes and sizes with various densities. They yield complex diffraction patterns and require more careful analyses and interpretations.

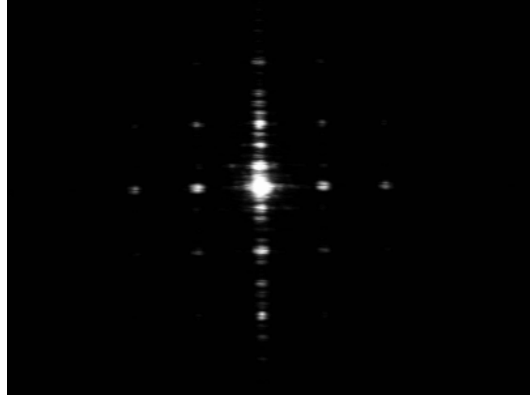


Figure 4. A typical diffraction pattern from a device wafer under laser beam irradiation perpendicular to the wafer surface.

Process Induced Strains as Characterized by the MRS-300

Microscopic Raman scattering is a powerful, nondestructive characterization method for both blanket and patterned Si wafers [6, 7]. Raman scattering does not require any additional sample preparation and provides various information of physical properties of materials. The crystal quality and degree of stress/strain of the crystal can be estimated from the full width at half maximum (FWHM) and shift of Raman peak from reference material. By selecting the wavelength of the excitation light source (laser), a measure of the crystal quality, stress and strain vs. depth can be obtained. In the case of an ideal and stress-free bulk crystal of Si, the Raman spectrum shows a single Lorentzian peak located at 520.3cm^{-1} with FWHM of $\sim 3\text{cm}^{-1}$ [8]. In reality, the peak usually broadens asymmetrically and shifts in frequency due to various factors such as residual stress, thermal expansion, lattice defect, crystal-size effect, etc.

We have designed a multi-wavelength Raman spectroscopy (MRS-300) system as an in-line stress/strain monitoring system. The system has three thermoelectrically cooled charge coupled device (CCD) cameras and can measure Raman peaks from three different excitation wavelengths without disturbing the set-up, (ie, without scanning the monochromator or switching the excitation laser). The system is capable of measuring 300mm wafers with a wavenumber resolution of $<0.1\text{cm}^{-1}$. A multi-line Ar^+ ion laser is used as a light source. Three lines (457.9, 488.0 and 514.5nm) of Ar^+ ion laser are used as the excitation source. In case of Si, the probe depth (one half of penetration depth) of Ar^+ ion laser is 140~350nm from the surface [8]. The Raman signals with shorter excitation wavelength provide material property information from the shallower region from the probed surface.

In this study, we have measured the Raman spectra of a Si peak from 300mm wafers after NiSi formation to estimate the effect of NiSi formation temperature on the stress/strain of Si wafers. Figure 5 shows the Raman spectra measured from various wafers after NiSi formation in the temperature range of 200~425°C. A longer wavelength (514.5nm) line of Ar⁺ laser was used as the excitation source. Raman shift and FWHM of Si peaks are summarized as a function of annealing temperature. The depth of the probed region is estimated from the absorption coefficient of the laser to be ~350nm.

As seen in Fig. 5, all the Si wafers showed a shift toward a higher wavenumber from bulk Si, regardless of NiSi formation temperature. As NiSi formation temperature increases, the peak continues to shift toward higher wavenumber side. Strain in Si is estimated to ~434MPa/cm⁻¹ [8]. The shift toward higher wavenumber side is caused by compressive stress. Based on the Raman measurement data, all wafers are under compressive stress (40~100MPa) and the stress increases as annealing temperature increases. The slope of the Raman shift rose at ~250°C, 315°C and 375°C, which suggests a high rate of compressive stress changes in Si near those temperatures due to the NiSi phase change. The FWHM of the peaks also show some correlation with the shift of peaks. The NiSi phase identification can be done by measuring Raman peaks in 100~250cm⁻¹. The identified NiSi phases are labeled in Fig. 5. For devices wafers, compressive stress up to ~400MPa (~1.0cm⁻¹ shift toward higher wavenumber side) was observed.

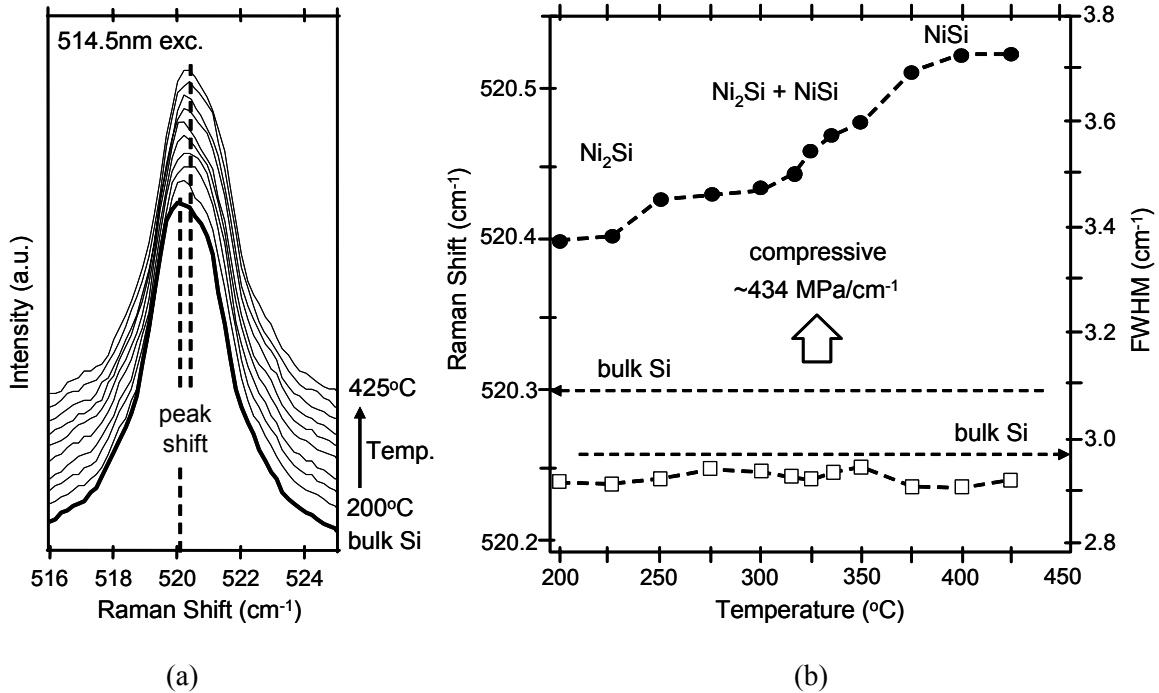


Figure 5. Raw Raman spectra from bare Si wafer and wafers after NiSi formation in the temperature range of 200~425°C (a) and summary of curve fitted spectra as a function of temperature.

Conclusions

Process induced local strain and/or deformation of surface flatness can cause focusing problems in photolithography steps and results in pattern overlay problems and critical dimension errors in nanometer scale devices. Global flatness is strongly desired for preventing pattern overlay problems in photolithography steps. Lattice strains can affect electrical properties of Si significantly. Understanding and managing process induced surface profiles and lattice strains are becoming extremely important for controlling nanometer scale device yields and performance and will be essential for future device fabrication processes.

In an effort to characterize process induced surface profiles and lattice strains, new non-destructive in-line process monitoring systems, optical surface profilometry (OSP) and multi-wavelength Raman spectroscopy (MRS) systems, have been developed. The process induced surface profiles and lattice strains, along with process results on 300mm blanket and device wafers before and after thermal processing, are characterized.

Optical surface profile and Raman characterization were performed on Ni films on 300mm p⁻-Si wafers with or without TiN capping layers before and after annealing, in addition to the conventional sheet resistance measurement using a four point probe. Quite significant changes in wafer surface profiles and strains near the Ni/Si interface were observed near phase transition (Ni/Si→Ni₂Si→NiSi→NiSi₂) temperatures determined by the temperature sensitivity curve of sheet resistance. It was experimentally verified that the wafer goes through global and local surface profile and strain (or stress) change during NiSi formation process step due to chemical reactions and physical changes under a given process environment.

References

1. T. Setokubo, E. Nakano, K. Aizawa, H. Miyoshi, J. Yamamoto, T. Fukada and W.S. Yoo, *Mat. Res. Soc. Symp. Proc.*, **810**, (2004) 259.
2. S.E. Thompson, G. Sun, K. Wu, J. Lim and T. Nishida, *IEDM* (2004) 221.
3. W.S. Yoo, T. Fukada and J. Yamamoto, *European Semiconductor*, (April (2001) 129.
4. W.S. Yoo and T. Fukada, *Electrochem. Soc. Proc.*, **PV 2000-9**, (2000) 355.
5. T. Murakami, T. Fukada and W.S. Yoo, *Electrochem. Soc. Proc.*, **PV 2002-11**, (2002) 253.
6. H. Harima, *Proc. 14th IEEE Int. Conf. on Advanced Thermal Processing of Semiconductors*, **RTP 2006**, (2006) 117.
7. M. Yoshimoto, H. Nishigaki, H. Harima, T. Isshiki, K. Kang and W.S. Yoo, *J. Electrochem. Soc.*, **153** (2006) G697.
8. S. Nishibe, T. Sasaki, H. Harima, K. Kisoda, T. Yamazaki and W.S. Yoo, *Proc. 14th IEEE Int. Conf. on Advanced Thermal Processing of Semiconductors*, **RTP 2006**, (2006) 211.